Van der Waals effects in ab initio water at ambient and supercritical conditions

Jonchiere, R ; Seitsonen, A P ; Ferlat, G ; Saitta, A M ; Vuilleumier, R

Abstract: Density functional theory (DFT) within the generalized gradient approximation (GGA) is known to poorly reproduce the experimental properties of liquid water. The poor description of the dispersion forces in the exchange correlation functionals is one of the possible causes. Recent studies have demonstrated an improvement in the simulated properties when they are taken into account. We present here a study of the effects on liquid water of the recently proposed semi-empirical correction of Grimme et al. J. Chem. Phys. 132, 154104 (2010)]. The difference between standard and corrected DFT-GGA simulations is rationalized with a detailed analysis upon modifying an accurate parameterised potential. This allows an estimate of the typical range of dispersion forces in water. We also show that the structure and diffusivity of ambient-like liquid water are sensitive to the fifth neighbor position, thus highlighting the key role played by this neighbor. Our study is extended to water at supercritical conditions, where experimental and theoretical results are much more scarce. We show that the semi-empirical correction by Grimme et al. improves significantly, although somewhat counter-intuitively, both the structural and the dynamical description of supercritical water.

DOI: https://doi.org/10.1063/1.3651474

Van der Waals effects in ab initio water at ambient and supercritical conditions

Romain Jonchiere, Ari P. Seitsonen, Guillaume Ferlat, A. Marco Saitta, and Rodolphe Vuilleumier

Citation: J. Chem. Phys. **135**, 154503 (2011); doi: 10.1063/1.3651474
View online: http://dx.doi.org/10.1063/1.3651474
View Table of Contents: http://jcp.aip.org/resource/1/JCPSA6/v135/i15
Published by the American Institute of Physics.

Van der Waals effects in *ab initio* water at ambient and supercritical conditions

Romain Jonchiere,[1,2] Ari P. Seitsonen,[3] Guillaume Ferlat,[1,a)] A. Marco Saitta,[1] and Rodolphe Vuilleumier[2]
[1]*UPMC, IMPMC, UMR CNRS−IPGP−UPMC n° 7590, 4 Place Jussieu, F-75252 Paris Cedex 05, France*
[2]*Ecole Normale Supérieure, Département de Chimie, UMR CNRS-ENS-UPMC n° 8640, 24, rue Lhomond, F-75005 Paris, France*
[3]*Physikalisch-Chemisches Institut der Universität Zürich, Winterthurerstrasse 190, CH-8057 Zurich, Switzerland*

(Received 28 July 2011; accepted 26 September 2011; published online 19 October 2011)

Density functional theory (DFT) within the generalized gradient approximation (GGA) is known to poorly reproduce the experimental properties of liquid water. The poor description of the dispersion forces in the exchange correlation functionals is one of the possible causes. Recent studies have demonstrated an improvement in the simulated properties when they are taken into account. We present here a study of the effects on liquid water of the recently proposed semi-empirical correction of Grimme *et al*. [J. Chem. Phys. **132**, 154104 (2010)]. The difference between standard and corrected DFT-GGA simulations is rationalized with a detailed analysis upon modifying an accurate parameterised potential. This allows an estimate of the typical range of dispersion forces in water. We also show that the structure and diffusivity of ambient-like liquid water are sensitive to the fifth neighbor position, thus highlighting the key role played by this neighbor. Our study is extended to water at supercritical conditions, where experimental and theoretical results are much more scarce. We show that the semi-empirical correction by Grimme *et al*. improves significantly, although somewhat counter-intuitively, both the structural and the dynamical description of supercritical water. [doi:10.1063/1.3651474]

I. INTRODUCTION

Liquid water is present everywhere and has a crucial role in many chemical, biological, or geological processes. A massive amount of experimental and theoretical studies has been carried out in order to understand the behavior of this fluid[1] but its properties at a microscopic scale remain somewhat elusive.[2] Although water is well described in a large range of thermodynamic conditions by a variety of existing classical potentials, a universal potential, able to provide a satisfactory description at all conditions or of all calculated properties, is still lacking; and the question of the transferability of potentials is thus always crucial. *Ab initio* molecular dynamics (AIMD), where atomic forces are calculated directly from first principles and the electronic structures, is conceptually free of these limitations but expensive in computational power. This problem is solved normally using the density functional theory (DFT) with generalized gradient approximation (GGA) or hybrid exchange-correlation functionals.

Unfortunately precedent studies of liquid water with this method,[3–17] give results which seriously differ from experimental data and even among each other. For example, radial distribution functions and self-diffusion coefficients within AIMD-GGA seemingly correspond to experimental results obtained at temperatures ∼20% lower than the simulated one. At first, a practical but empirical solution was to some extent successfully employed, namely to perform simulations at temperatures 20% higher than the target one. However, this approach cannot be considered satisfying for a detailed description and understanding of water properties.

The origin of the differences between AIMD-GGA and experiments is still unclear: the poor description of the dispersion forces in the GGA functionals is one of the hypothesis but the neglect of quantum nature of the nuclei is another possible explanation. On one hand, the latter assumption has been studied in liquid water by Chen *et al*.,[18] Schwegler *et al*.,[5] and Morrone and Car.[19] They suggest that the quantum effects influence the structure and diffusion of the water, but their extent remains unclear.

On the other hand, different approaches have been used to include the dispersion forces in DFT-GGA, such as "pure" density (DF) (Ref. 20) or nonlocal van der Waals (vdW-DF) functionals,[21–25] self-consistent polarization density functional theory (SCP-DFT),[26] maximally localized Wannier functions,[27,28] semi-empirical C_6R^{-6} potential corrections (DFT-D),[29–34] or modifications in the pseudopotentials, as in the dispersion-corrected atom-centered potentials (DCACP) scheme.[35,36] Calculations performed with these different methods in the case of the water in clusters[37–39] or bulk[16,40–43] systems clearly show that the dispersion forces provide a significant improvement in the simulated properties. Recent work of Wang *et al*.,[42] using vdW-DF of Dion *et al*.,[22] highlights the role of anti-tetrahedral structures to explain the improvement of the structure and the self-diffusion.

In this study we employ the latest semi-empirical parameterisation of "DFT-D" scheme proposed by Grimme *et al*. in

a)Author to whom correspondence should be addressed. Electronic mail: guillaume.ferlat@impmc.upmc.fr.

2010 (Ref. 34) (Grimme-D3) to model the London dispersion interactions in liquid water at ambient-like conditions simulated with BLYP exchange-correlation functional.[44,45] In parallel, we have modified a popular classical potential to estimate the range and effects of the dispersion forces in classical simulations and to compare them with the AIMD results. We confirm the conclusions of Wang *et al.*,[42] and we show that the fifth neighbor is a key observable for the structure and self-diffusivity of the ambient liquid water. Finally, the transferability of this correction is studied with simulations of water at supercritical-like conditions, where Grimme-D3 correction similarly improves the structural and dynamical results.

II. METHODS

A. *Ab initio* molecular dynamics

1. Computational details

We carried out AIMD-DFT calculations using a hybrid Gaussian plane-wave method[46] as implemented in the QUICKSTEP/CP2K code.[47,48] This approach combines a Gaussian basis set for the wave functions with an auxiliary plane wave (PW) basis set for the density. We chose a triple-zeta valence doubly polarized basis set since it has been shown to provide a good compromise between accuracy and computational cost.[9] After tests, listed in the Appendix on the parameters of the plane-wave grid we chose to use a charge density cutoff of 400 Ry and NN50 smoothing. Core electrons were replaced by the Goedecker-Teter-Hutter norm-conserving pseudopotentials.[49,50] The BLYP approximation[44,45] is one of the most widely used exchange-correlation (XC) functionals to describe liquid water. We thus use it as a representative of typical DFT-GGA accuracy in this work.

We took the London dispersion interactions into account using the scheme proposed recently by Grimme and coworkers and hereafter called Grimme-D3.[34] In this approach, the total energy as obtained from the usual self-consistent Kohn-Sham XC (BLYP) is supplemented by a dispersion correction energy (E_{disp}) which is a sum of two- and three-body inter-atomic terms. The analytical form of these terms, varying as r^{-n} (n = 6, 8, ...) and r^{-3} in the two-body and three-body terms, respectively, is determined by calculating the interaction coefficient in a first-principles manner, and fitting the two residual parameters to high-level, beyond DFT, *ab initio* data. In our calculations, the two-body terms are limited to n = 6 and n = 8 contributions. Simulations restricted to two-body terms only are hereafter referred to as BLYP-D3(2b). We also investigate the influence of the three-body terms in calculations taking also the corresponding term into account; these calculations are denoted as BLYP-D3.

Born-Oppenheimer molecular dynamics simulations were carried out in the NVT ensemble with a Nosé-Hoover thermostat chain, yielding trajectories from 50 up to 120 ps (see Table I) with a time step of 0.5 fs. Two different thermodynamic points were investigated that we shall refer to, in the following, as ambient- and supercritical-like conditions. They correspond to temperature–density of 323 K–1.00 g cm^{-3} and 673 K–0.58 g cm^{-3}, respectively. Our systems contain 128 D_2O molecules in periodic cubic boxes of length 15.746 (ambient-like) and 18.754 Å (supercritical-like). For the sake of testing the DFT potential energy surfaces, one would like to simulate the absolute experimental temperatures (i.e., 298 K at ambient). However, the rationale for targeting the temperature 323 K for the ambient-like conditions is to prevent the effect of slow dynamics on the phase-space sampling. The initial configurations for the *ab initio* simulations were taken from classical simulations. Water properties were analysed after an equilibration time of 20 ps at ambient-like and 10 ps at supercritical-like conditions. A the end of the runs, the effective temperature has been calculated from the velocities self-correlation functions.

TABLE I. Summary table of our *ab initio* simulations: temperature (T), equivalent light-water density (ρ), method and duration of the trajectory.

T (K)	ρ (g cm^{-3})	Method	Duration (ps)
317	1.00	BLYP	57
322	1.00	BLYP-D3(2b)	126
322	1.00	BLYP-D3	122
684	0.58	BLYP	51
659	0.58	BLYP-D3(2b)	92
668	0.58	BLYP-D3	107

B. Classical molecular dynamics

In order to obtain a deeper understanding of the role and characteristic length of London dispersion interactions in AIMD calculations, we also carried out classical molecular dynamics (MD) simulations. In this case, since typical model potentials intrinsically contain the long-range vdW interactions, their progressive suppression can provide an interesting comparison with respect to BLYP results. To this end, we chose a popular pair-potential, TIP4P/2005,[51] which is given by the sum of a Coulomb and a Lennard-Jones (LJ) term. We modified the attractive r^{-6} part of the latter term, which in the chosen model only acts between oxygen atoms, by using a cutoff function (f_c^{ij}) as follows:

$$E_{\text{LJ}}^{c} = \sum_{i,j}^{i<j} 4\epsilon_{ij}\left[\left(\frac{\sigma_{ij}}{r_{ij}}\right)^{12} - f_c^{ij}\left(\frac{\sigma_{ij}}{r_{ij}}\right)^{6}\right], \tag{1}$$

where the cutoff function, similar to the damping function used in Ref. 32, reads as

$$f_c^{ij}\left(\frac{r_{ij}}{r_c^{ij}}\right) = 1 - \frac{1}{1+\exp\left[-d\left(\frac{r_{ij}}{r_c^{ij}}-1\right)\right]}. \tag{2}$$

Here $d = 20$; $f_c^{ij}(r) \simeq 1$ if $r \ll r_c^{ij}$ and $f_c^{ij}(r) \simeq 0$ if $r \gg r_c^{ij}$. r_c^{ij}, the cutoff radii, has been modified in a large range to study its influence on structure and dynamics. Simulations were performed with oxygen-oxygen LJ cutoff radius r_c^{OO} ranging from 2.5 to 8.0 Å and then with the non-modified Lennard-Jones potential, which corresponds to $r_c^{\text{OO}} = \infty$.

The classical molecular dynamics calculations were carried out in the NVT ensemble with Nosé-Hoover thermostat chain using the DLPOLY V2.2 code.[52] The trajectories were

run for 10 ns with a time step of 1 fs. Water properties were collected and calculated after an equilibration time of 200 ps. Our systems contain 1024 H_2O molecules in periodic cubic boxes of length 31.492 and 37.509 Å, corresponding to the same ambient-like and supercritical-like AIMD densities, and the temperatures are also the same in the classical MD and AIMD simulations.

III. RESULTS AND DISCUSSIONS

A. Ambient-like conditions

1. *Ab initio* study of the Grimme-D3 correction

Oxygen-oxygen (g_{OO}'s) and oxygen-hydrogen (g_{OH}'s) radial distribution functions obtained from the simulations are presented in Figure 1 along with the experimental results.[53] The relevant maxima and minima of the g_{OO}'s are collected into Table II.

The radial distribution functions obtained with BLYP show significant overstructuring compared to the experimental data, in agreement with the previous standard BLYP results.[6,8,9] In contrast, simulations with the Grimme-D3 correction yield g_{OO} and g_{OH} that are less structured (see Table II)

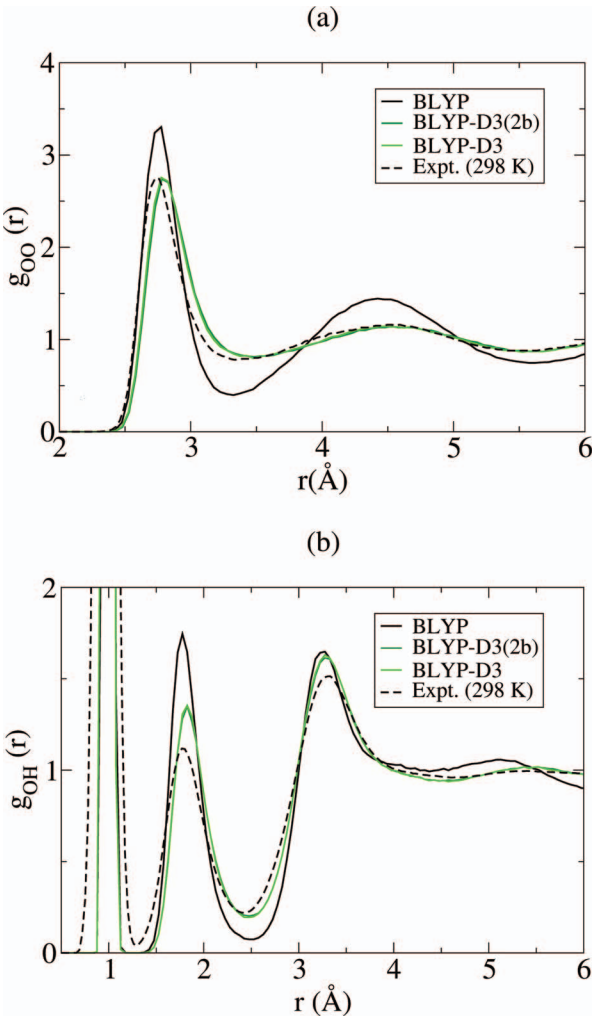

FIG. 1. (a) Oxygen-oxygen (g_{OO}) and (b) oxygen-hydrogen (g_{OH}) radial distribution functions obtained from the different methods and from experimental neutron scattering data (Ref. 53) at ambient-like conditions.

TABLE II. Maxima (g_{OO}^{max}I, g_{OO}^{max}II) and minima (g_{OO}^{min}I) values of the g_{OO} obtained from the different methods and from experimental neutron scattering data (Ref. 53) at ambient-like conditions.

Method	T (K)	g_{OO}^{max}I r ≃ 2.8 Å	g_{OO}^{min}I r ≃ 3.4 Å	g_{OO}^{max}II r ≃ 4.5 Å
BLYP	317	3.30	0.40	1.44
BLYP-D3(2b)	322	2.74	0.81	1.14
BLYP-D3	322	2.76	0.80	1.14
Expt. D_2O[a]	298	2.75	0.78	1.16

[a]Reference 53.

than BLYP, and thus significantly closer to neutron scattering experimental data.[53] We note that the effect of the three-body term within the Grimme-D3 correction (referred to as BLYP-D3) is very marginal.

Self-diffusion coefficients (D) calculated with the Einstein and Green-Kubo formulas give very similar results (see Table III).

Our estimate of D in BLYP heavy water at $T = 323$ K is very small ($D \simeq 0.01$–0.03 Å^2 ps^{-1}) compared to the experimental value[54] at $T = 318$ K ($D = 0.30$ Å^2 ps^{-1}). Finite-size effects affecting the numerical results must, however, be taken into account when performing this comparison. These corrections are inversely proportional to the length of the cell and to the viscosity. Since the latter quantity is unknown in our calculations, we instead follow Ref. 14, where the experimental result is adjusted to represent a hypothetical periodic system of 128 water molecules. We obtain modified values of 0.24 Å^2 ps^{-1} at 318 K. Thus, even accounting for this modification, the diffusion in BLYP water remains clearly underestimated. This is in line with the observed overstructuring (Figure 1). The Grimme-D3 correction provides a significant improvement ($D = 0.17$ Å^2 ps^{-1}), analogously to the results (0.21–0.26 Å^2 ps^{-1}) obtained with other London dispersion-corrected functionals.[40,42] However, the obtained value still

TABLE III. Self-diffusion coefficients obtained with the Einstein (D_{Einst}) and Green-Kubo (D_{GK}) formula compared with experimental data and other studies at ambient-like conditions. The experimental values have not been modified for the finite size effects here (see text).

Method	T (K)	D_{Einst} (Å^2 ps^{-1})	D_{GK} (Å^2 ps^{-1})
BLYP	317	0.01	0.03
BLYP-D3(2b)	322	0.16	0.17
BLYP-D3	322	0.17	0.16
BLYP-DCACP[a]	325	0.21	
DRSLL-PBE[b]	303	0.21	
DRSLL[b]	300	0.26	
Expt. D_2O[c]	298	0.19	
Expt. D_2O[d]	303	0.21	
Expt. D_2O[c]	318	0.30	
Expt. H_2O[e]	298	0.23	
Expt. H_2O[e]	318	0.36	

[a]Reference 40.
[b]Reference 42.
[c]Reference 54.
[d]Reference 55.
[e]Reference 56.

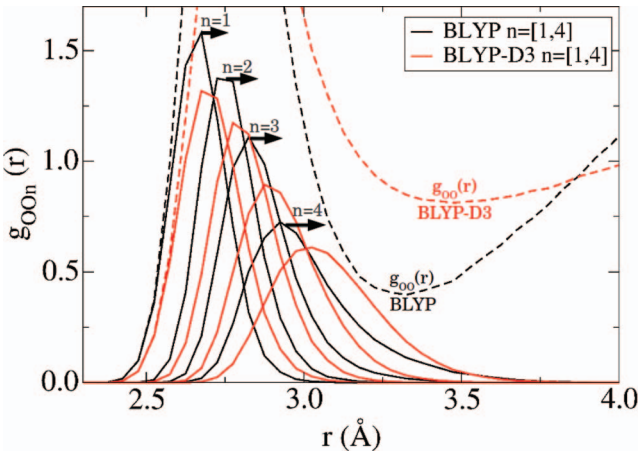

FIG. 2. Oxygen-oxygen radial distribution functions (g_{OO_n}) of neighbors for n=1 to 4 [1, 4] obtained from BLYP and BLYP-D3 simulations at ambient-like conditions.

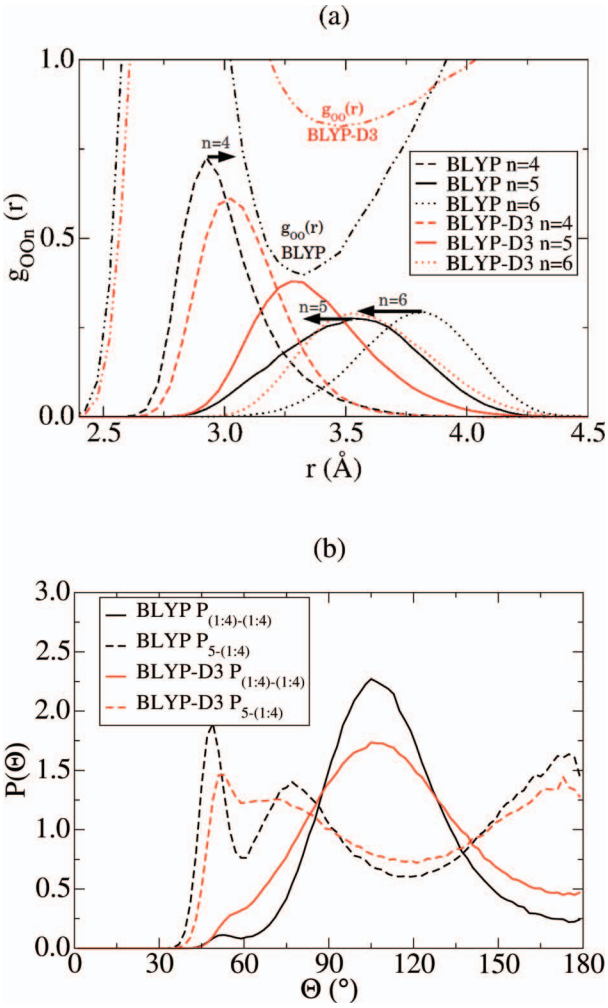

FIG. 3. (a) Oxygen-oxygen radial distribution functions (g_{OO_n}) of 4th, 5th, and 6th neighbors and (b) average oxygen-oxygen angular distribution functions ($P(\theta)$) between the first four neighbors ($P_{(1:4)-(1:4)}(\theta)$) and between the first four neighbors and the 5th neighbor ($P_{5-(1:4)}(\theta)$) obtained from BLYP and BLYP-D3 simulations at ambient-like conditions.

underestimates the experimental one, meaning that a temperature shift is still needed for BLYP-D3 water to be as diffusive as real water. This is consistent with the recent work of Yoo and Xantheas.[43]

In order to gain further insight, we proceeded to a detailed local structural analysis of BLYP and BLYP-D3 water. At each molecular dynamics configuration, the nearest neighbors of each water molecule were determined and ordered according to their distances. By averaging over all the configurations and water molecules, oxygen-oxygen radial distribution functions of each nth neighbor, hereafter called g_{OO_n}, were calculated. See, e.g., Refs. 57 and 58 for similar analysis in water and amorphous ices.[59]

Figure 2 shows the obtained g_{OO_n} for first tetrahedral shell neighbors (n = 1–4). One can note that in BLYP-D3 water the first coordination shell is shifted outwards with respect to BLYP water, which of course results in a broader and less pronounced g_{OO} first peak (Figure 1). Note that this corresponds to an increase of only 1% in the average distances (d_{OO_n}). The g_{OO} second peak is also less pronounced since the corresponding neighbors (n = 5–24) are more uniformly distributed and over a larger *r*-range (not shown). These destructuring effects can be explained in term of mutual, non-hydrogen-bonded attraction among molecules belonging to different shells, which partly compensated the stronger hydrogen bonding properties of BLYP water. The influence of the London dispersion correction is especially noticeable in the fifth- and sixth-neighbor distributions. Indeed, these distributions are shifted by 0.15 Å to smaller distances in BLYP-D3 compared to BLYP (see Figure 3(a)). Thus, these neighbors with BLYP-D3 fall in the region of the first minimum (3.3–3.5 Å) of BLYP, resulting in a less marked distinction between the first and second shell of neighbors.

Using the neighbors indexation, angular distribution functions formed by a water molecule and two of its nth neighbors, $P_{i-j}(\theta)$, can be constructed. The average over all the triplets involving neighbors inside the first coordination shell is thus defined by $\langle P_{(1:4)-(1:4)}(\theta)\rangle = 1/6 \sum_{i,j=1,i<j}^{4} P_{i-j}(\theta)$. As seen in Figure 3(b), this distribution peaks at around $\theta = 109°$, i.e., close to the tetrahedral angle. By considering the triplets which involve the 5th and any of the first four neighbors, we define $\langle P_{5-(1:4)}(\theta)\rangle = 1/4 \sum_{i=1}^{4} P_{5-i}(\theta)$. The value of this quantity implies (cf. Figure 3) that the fifth neighbor preferentially occupies anti-tetrahedral positions at $\theta = 180°$ and $\theta \simeq 70°$, the peak at about 45° being due to steric effects. This is the case in both BLYP and BLYP-D3 calculations, although in the latter case all the peaks are less marked, revealing a more disordered angular structure.

The geometric criteria, $r_{OO} < 3.5$ Å and $\angle_{OH-O} < 30°$, for a hydrogen bond were chosen to evaluate the number of hydrogen bonds (HB) per molecule distribution (see Figure 4(a)). An average number of HB of 3.80 and 3.68 is obtained with BLYP and BLYP-D3, respectively. This difference is essentially due to the ratio between the four-fold and the three-fold HB configurations decreasing from about 4:1 with BLYP to 2:1 with BLYP-D3.

The vibrational spectra (see Figure 4(b)) obtained from the velocity auto-correlation functions are a complementary source of information regarding hydrogen bonding. Four peaks are observed, at around 70 340 (libration), 1080

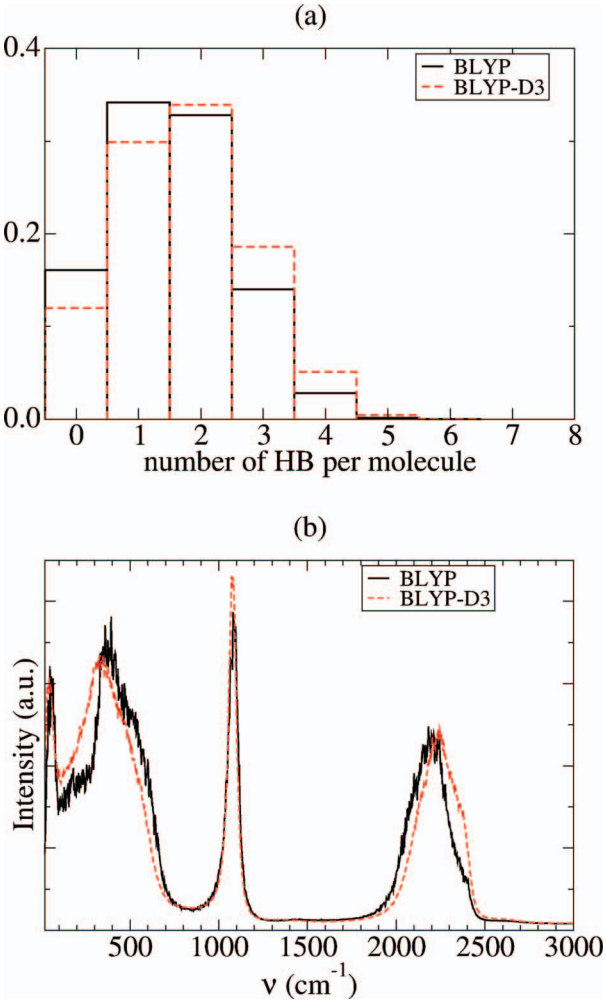

FIG. 4. (a) Distribution of number of hydrogen bonds per molecule and (b) vibrational spectra of heavy water obtained from BLYP and BLYP-D3 simulations at ambient-like conditions.

(D-O-D bending), and 2230 (O-D stretching) cm^{-1}. BLYP-D3 results slightly differ from BLYP ones on the O-D stretching peak ($\nu \simeq 2240\ cm^{-1}$ vs $\nu \simeq 2210\ cm^{-1}$) and on the second libration peak ($\nu \simeq 330\ cm^{-1}$ vs $\nu \simeq 375\ cm^{-1}$) frequencies. These slight shifts in BLYP-D3 results indicate a weaker hydrogen-bonded network.

Thus, all the obtained results give a consistent picture. With the Grimme-D3 correction, the first shell of neighbors is more perturbed by the presence of the fifth neighbor. The hydrogen-bonded network is thus weaker, which explains the increase in the self-diffusion coefficient.

2. Classical molecular dynamics study of dispersion forces

Ten simulations at different cutoff radii, r_c^{OO}, have been performed at T = 323 K. The properties of each simulated water sample were compared with the ones of the non-modified potential.

We observe three different behaviors of the oxygen-oxygen radial distribution function (g_{OO}): results at representative radii are shown in Figure 5. At $r_c^{OO} > 4$ Å, there is

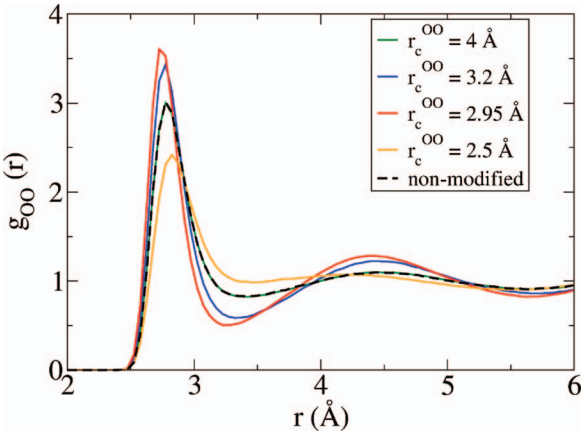

FIG. 5. Oxygen-oxygen radial distribution functions (g_{OO}) obtained at ambient-like conditions from the simulations using the non-modified potential and the modified potentials with a cutoff radius (r_c^{OO}) of 4.0, 3.2, 2.95, and 2.5 Å.

no noteworthy difference in the g_{OO} compared to the non-modified potential. Indeed, Lennard-Jones interactions are practically negligible beyond these distances. At $r_c^{OO} < 2.7$ Å, the g_{OO} is less structured than with the non-modified potential. The cutoff radius is (unphysically) smaller than the average nearest-neighbor distance from d_{OO_1} and all molecules are further away from one another. Finally, for r_c^{OO} between 2.7 and 4 Å, the g_{OO} is over-structured, similar to the standard BLYP results.

The self-diffusion coefficient (D) obtained at $r_c^{OO} = 6$ Å (and with the non-modified potential) is 0.35 $Å^2\ ps^{-1}$. D slightly increases with decreasing cutoff radius until $D = 0.40\ Å^2\ ps^{-1}$ at $r_c^{OO} = 3.7$ Å (see Figure 6). A sharp decrease in D is observed at r_c^{OO} values between 2.7 and 4.0 Å with a minimum of $D = 0.14\ Å^2\ ps^{-1}$ obtained at $r_c^{OO} = 2.95$ Å. At smaller r_c^{OO}, D continues to increase. Interestingly, the overstructuring of the g_{OO} and the decrease of D are most pronounced at the same cutoff radius, $r_c^{OO} = 2.95$ Å.

The behavior obtained at $r_c^{OO} = 2.95$ Å (overstructuring and lower diffusivity) is qualitatively similar to the one obtained with BLYP in AIMD. In the same way, the

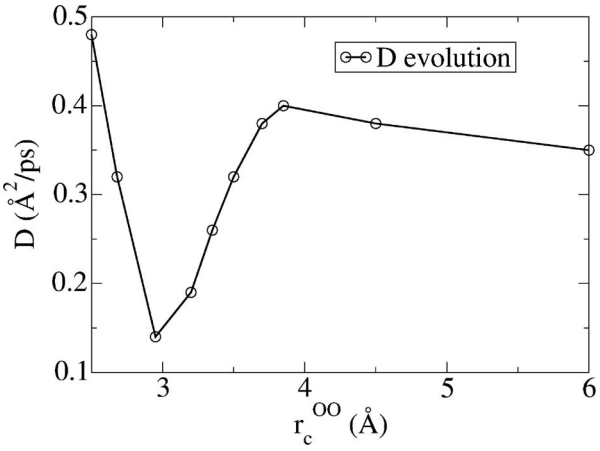

FIG. 6. Evolution of the self-diffusion coefficient (D) obtained from the simulations using a modified potential as a function of the cutoff radius (r_c^{OO}).

behavior obtained with the non-modified potential and at the *ab initio* level with the Grimme-D3 correction is similar, as expected. This is illustrated in Figure 7(a). Thus, the suppression of the dispersion forces in the classical potential with respect to the full potential can be described as the direct counterpart of the absence of dispersion forces in AIMD. To confirm this qualitative picture, we analyse in more details the structure obtained from the classical simulations using $r_c^{OO} = 2.95$ Å, which will be denoted as modified-MD, and the non-modified MD potential. The results are compared with the *ab initio* ones in Figure 7.

The two maxima in g_{OO} are much higher in modified-MD water (Figure 7(a)) than in the non-modified MD. At $r_c^{OO} = 2.95$ Å, the first four average distances (d_{OO_n}) shorten by about 1.5%. The second shell neighbors (n = 5–24) contract around the mean distance of the 12th neighbor, $d_{OO_{12}} = 4.47$ Å, from [3.40 Å ; 5.62 Å] in MD to [3.50 Å; 5.60 Å] in modified-MD (not shown). The fifth neighbor average distance is shifted from 3.40 to 3.50 Å at a distance fully within the second coordination shell (Figure 7(b)). More interestingly, the fifth neighbor distance distributions indicate a clear analogy between ordinary BLYP and modified-MD on one hand, and between London dispersion-corrected BLYP and non-modified MD on the other hand. This analogy is further supported by finer structural data such as the orientational correlations. The oxygen-oxygen angular distribution function ($P(\theta)$) confirms the weaker interaction between the two shells. In modified-MD, such as in BLYP water, the first four neighbors have a clear tetrahedral geometry, whereas the fifth neighbor is more localized at the anti-tetrahedral positions $\theta = 180^\circ$ and $\theta = 70^\circ$ (Figures 7(c) and 7(d)).

Our analysis, thus, sheds new light on the validity of DFT-based simulations of bulk water at ambient conditions. Even if the position in the phase diagram is different in *ab initio* and classical simulations, our results clearly indicate that BLYP water is analogous, from both the structural and the diffusive points of view, to studying classical water with a LJ potential truncated at *shorter* distances than the LJ potential well.

B. Supercritical-like conditions

At supercritical-like conditions, in analogy with the results at ambient-like conditions, BLYP-D3 simulations give

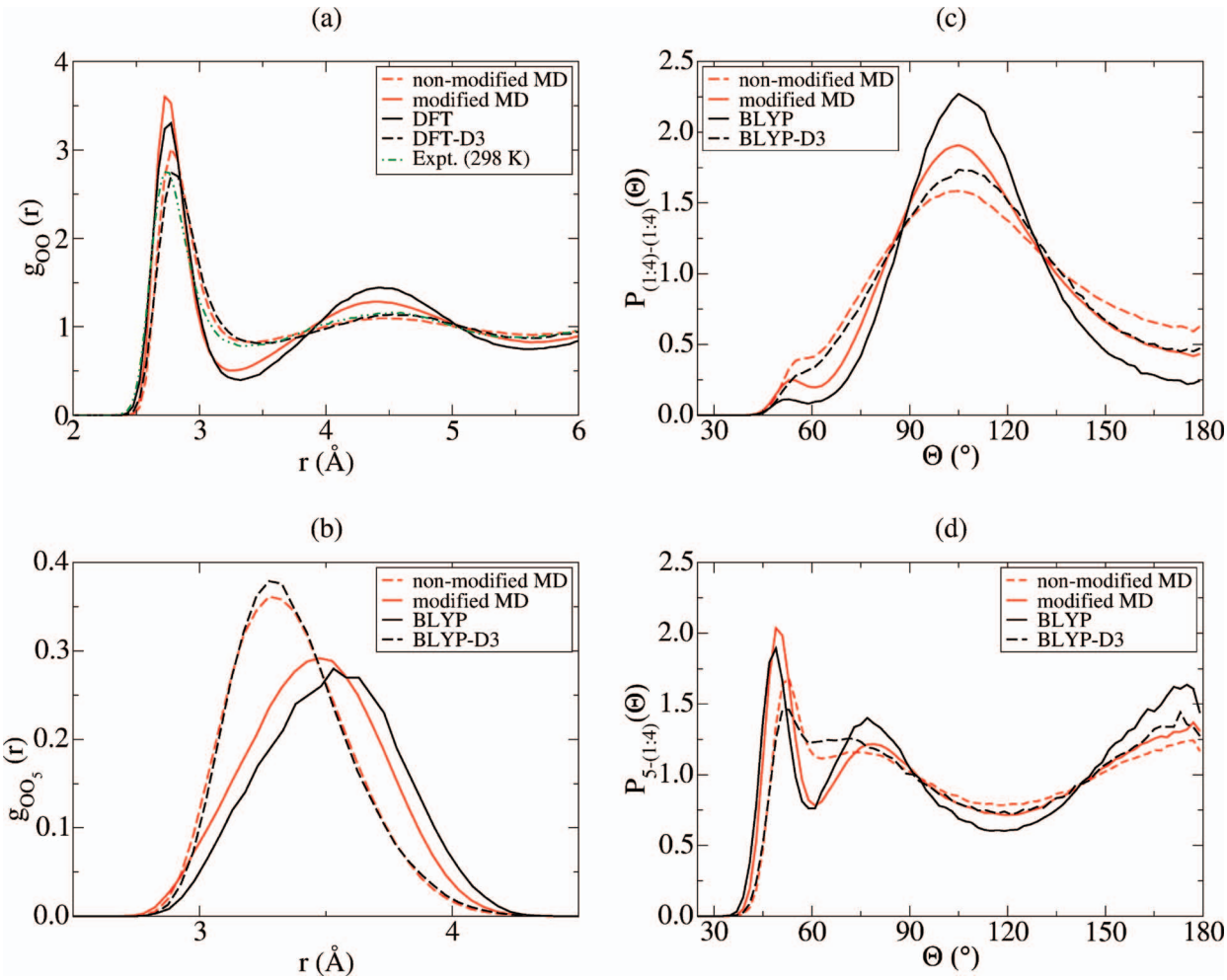

FIG. 7. Comparison of classical and *ab initio* simulation results obtained with (non-modified MD and BLYP-D3) or without (modified MD and BLYP) dispersion forces in ambient-like liquid water. (a) Oxygen-oxygen radial distribution functions (g_{OO}). (b) Oxygen-oxygen radial distribution functions of 5th neighbor (g_{OO_5}). (c) Average oxygen-oxygen angular distribution functions of the angles between the first four neighbors ($P_{(1:4)-(1:4)}(\theta)$). (d) Average oxygen-oxygen angular distribution functions of the angles between the first four neighbors and the 5th neighbor ($P_{5-(1:4)}(\theta)$).

TABLE IV. Self-diffusion coefficients obtained with the Einstein (D_{Einst}) and Green-Kubo (D_{GK}) formula compared with experimental data at supercritical-like conditions.

Method	T (K)	D_{Einst} (Å^2 ps^{-1})	D_{GK} (Å^2 ps^{-1})
BLYP	684	5.1	5.2
BLYP-D3(2b)	659	4.2	4.0
BLYP-D3	668	4.6	4.5
Expt. H_2O[a]	673	5.7	
Expt. D_2O[b]	623	4.4	

[a]Reference 63.
[b]Reference 55.

almost identical results with BLYP-D3(2b), see for instance Table IV. This confirms that the three-body contributions in Grimme-D3 are negligible in the studied range of pressures and temperatures. Thus, in the following we will only present the results obtained with BLYP and BLYP-D3, comparing to experimental data whenever available.

1. Ab initio study of van der Waals effects

The oxygen-oxygen radial distribution functions (g_{OO}) are shown in Figure 8. The maximum in g_{OO} at ~3 Å is more pronounced with BLYP-D3 than with BLYP. This is in contrast with the ambient case where the opposite situation is observed. A second peak, hardly present with BLYP, is clearly visible with BLYP-D3.

Compared to the experimental data[60] both *ab initio* results yield the first peak at a larger radius, but BLYP-D3 is in significantly better agreement than BLYP. At distances between 5 and 7 Å, there is no visible second peak in the experimental data. This latter difference, however, might well be below the poorer experimental accuracy at these extreme conditions. Indeed, one should keep in mind that the partial distribution functions of Ref. 60 are affected by uncertainties arising from different sources. In particular, the contribution from the oxygen-oxygen partial to the total neutron scattering data is about 1%, due to the strong neutron absorption resulting from the high-pressure experimental setup. In an attempt to reduce the artefacts in the analysis of the experimental data arising from a Fourier transformation, we compare in Figure 9 the neutron total structure factors calculated from our configurations with the experimental one.[60]

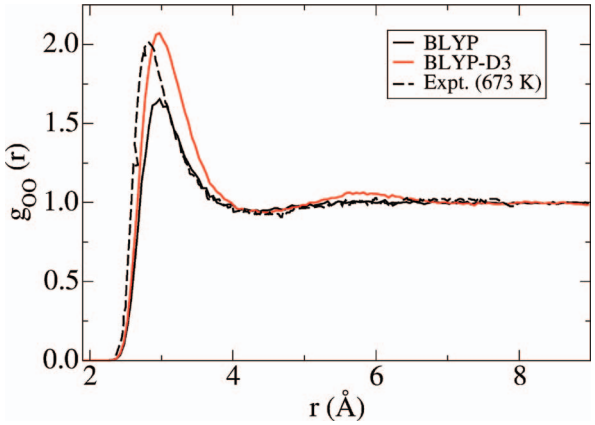

FIG. 8. Oxygen-oxygen radial distribution function (g_{OO}) calculated from the BLYP and BLYP-D3 simulations and from experiments[60] at supercritical-like conditions.

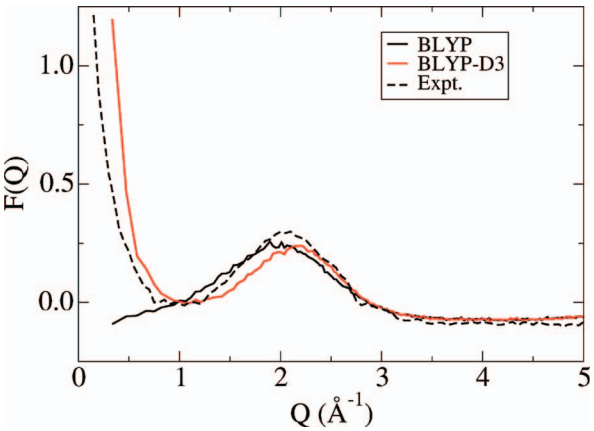

FIG. 9. Neutron total structure factor ($F(q)$) calculated from the BLYP and BLYP-D3 simulations and from experiments[60] at supercritical-like conditions.

At Q below 1 Å^{-1}, both the experimental and BLYP-D3 results show a strong increase in the signal which is not observed with BLYP. The Q = 0 Å^{-1} limit can be computed from the compressibility of the system[61] and it is found to be 1.28 using the value of the compressibility of water at 673 K and 500 bars.[62] This value is consistent with the low Q experimental data. The increase in the signal at low Q with BLYP-D3 is thus in good agreement with the experimental behavior, contrary to the BLYP data. We believe that the inability of BLYP to catch the strong low-Q increase points to a significant deficiency which is corrected, if not over-corrected, by BLYP-D3.

The self-diffusion coefficients (D) are presented in Table IV. The self-diffusion coefficient in BLYP heavy water at 673 K (D = 5.2 Å^2 ps^{-1}) is very close to the experimental values at the same temperature[55,63] (D = 5.7 Å^2 ps^{-1}). Use of the Grimme-D3 correction gives a smaller value (D = 4.6 Å^2 ps^{-1}). A similar trend is observed in the classical simulations: D = 5.5 Å^2 ps^{-1} for modified-MD versus D = 4.4 Å^2 ps^{-1} for non-modified MD.

As it could be anticipated from the absence of well-defined minima in the g_{OO}, the nearest neighbors are almost continuously distributed (Figure 10(a)), showing no clear coordination shells. The effect of the dispersion correction (BLYP-D3) is to shorten the average distance of each neighbor distribution.

The angular distribution functions ($P_{i-j}(\theta)$) from BLYP and BLYP-D3 simulations (see Figure 10(b)) confirm the loss of the tetrahedral geometry: only the first two (or three) neighbors show a reminiscence of the tetrahedral angle distribution. The intensity of this peak shows tiny differences between different simulations: while the first two neighbors are more localized with BLYP than BLYP-D3, the inverse is the case for the third one.

The hydrogen bonding connection has been calculated (Figure 11(a)) using the geometric criteria used previously.

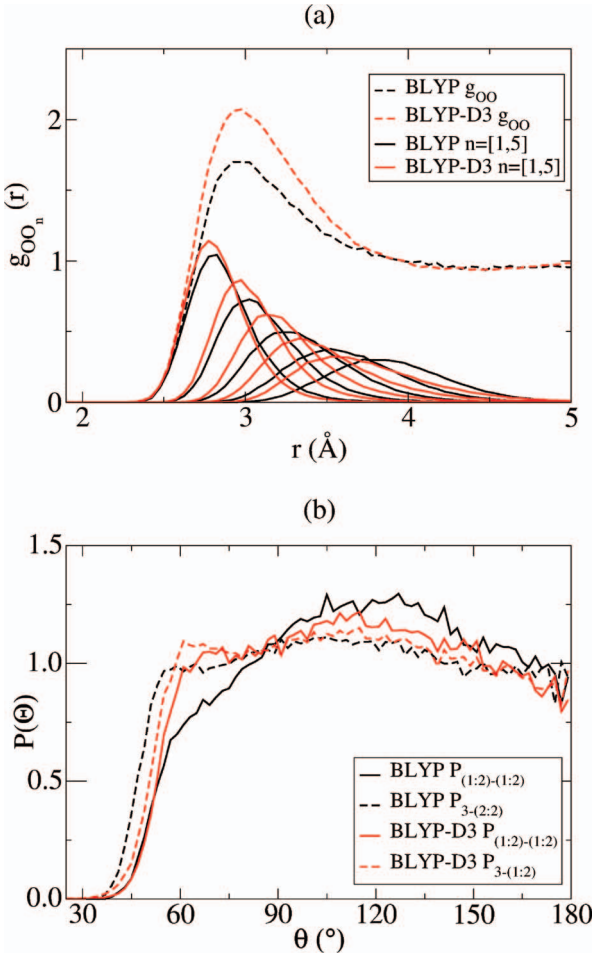

FIG. 10. (a) Oxygen-oxygen radial distribution functions of the first five neighbors (g_{OO_n}) and (b) average oxygen-oxygen angular distribution functions ($P(\theta)$) of the angles between the two first neighbors (1-2) and the angles between the first two neighbors and the 3rd neighbor (i-3) obtained from BLYP and BLYP-D3 simulations at supercritical-like conditions.

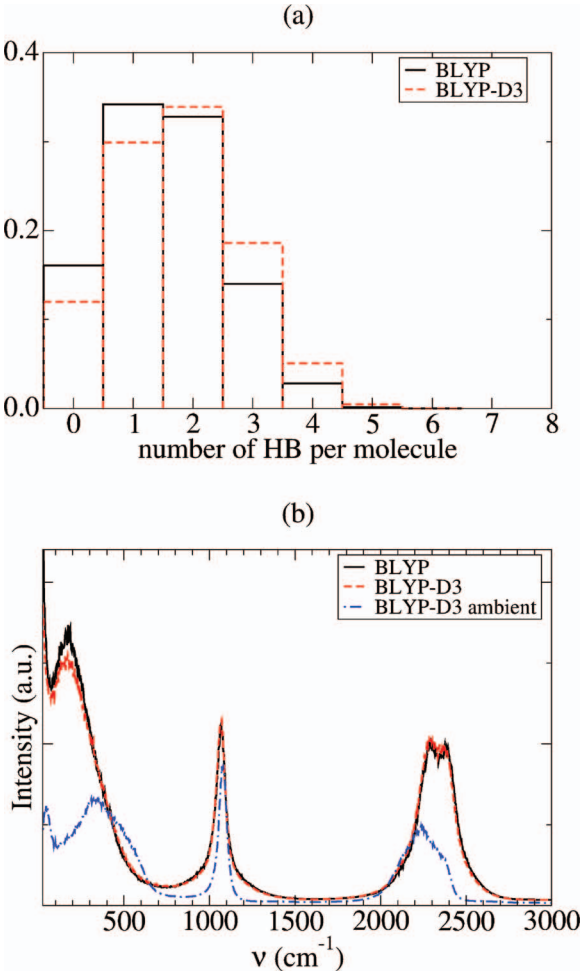

FIG. 11. (a) Distribution of number of hydrogen bonds per molecule and (b) vibrational spectra of heavy water obtained from BLYP and BLYP-D3 simulations at supercritical-like conditions.

At supercritical conditions, most of the molecules have either one (≃30%) or two (≃30%) HB. There is a finite number of molecules having no HB at all (≃15%), in contrast to the ambient situation. The HB average number per molecule is markedly reduced at supercritical conditions compared to the ambient ones: from about 3.80 to 1.56 with BLYP. Addition of the Grimme-D3 correction tends to increase the average number of HB per molecule, from 1.56 with BLYP to 1.76 with BLYP-D3. At supercritical conditions most water molecules are not HB saturated and thus free to create (instantaneous) new HB. As a result, the decrease of the average distance to the nearest neighbors with BLYP-D3 (Figure 10(a)) allows for a slightly larger number of HB.

Compared to the vibrational spectra obtained at ambient conditions, libration peaks are shifted (see Figure 11(b)) to lower (20 and 160 cm^{-1} vs 70 and 340 cm^{-1}) and O-D stretching peaks to higher frequencies. The D-O-D bending frequency is less affected, with a shift from 1080 to 1065 cm^{-1}. These shifts can be interpreted in terms of a weakening of hydrogen-bonds.

IV. CONCLUSIONS

We have performed AIMD calculations of liquid water at ambient-like and supercritical-like conditions with pure BLYP functional and BLYP with Grimme-D3 correction. Classical molecular dynamics simulations have been carried out using different potentials with or without dispersion forces to provide a simple yet informative interpretation of London dispersion correction (or lack thereof) in the DFT-GGA study of liquid water. In particular, we have shown that standard BLYP is similar to classical MD simulations carried out with a model potential where the LJ interaction is truncated beyond an unrealistic short distance.

We observed that the structural and diffusive properties of water are significantly better described with respect to experiments if Grimme-D3 correction is included than in ordinary BLYP water. At ambient-like conditions, the BLYP-D3 structure is softer because of a more uniform spatial distribution of the neighbors. Improvement of the diffusion is explained by the location of the fifth and sixth neighbors as bridges between the first and the second shell of coordination. These neighbors, very localized at the anti-tetrahedral positions in BLYP water, are closer to the first four tetrahedral neighbors with Grimme-D3 correction. This displacement creates

a more disorganized configuration where the hydrogen-bonds are weaker and the different shells of neighbors are less separated, resulting in an easier diffusion of water molecules. Finally, our preliminary study of water at supercritical-like conditions indicates the Grimme-D3 correction to BLYP has an opposite effect with respect to ambient-like conditions, but even in this case the agreement with experiments is improved.

ACKNOWLEDGMENTS

We thank A. K Soper and M. A. Ricci for providing us with the experimental data of Ref. 60. We also thank Joost VandeVondele and Jürg Hutter for various discussions. This work was performed using HPC resources from GENCI-CINES/IDRIS (Grant No. x2011082309).

APPENDIX: CHARGE DENSITY CUTOFF AND CONVERGENCE

The convergence of the auxiliary PW basis set is controlled by a charge density cutoff. While a relatively low cutoff of 280 Ry has commonly been used in liquid water,[43] the importance of large and well-converged basis-sets has been pointed out.[12] We thus investigated the effect of the PW cutoff on the geometry and energetics of water dimers and then on the bulk liquid properties.

In liquid water, because of the disorder, configurations far from the optimal hydrogen-bond arrangement can contribute to the observed properties. For this reason, two characteristic dimer configurations (attractive and purely repulsive) are commonly used to benchmark the interaction energy curves.[40] Both configurations have been obtained from the TIP4P/2005 monomer geometry:[51] the monomers geometry being fixed, the only degree of freedom is the O-O distance (r_{OO}) between the monomers.

The interaction energy curves (see Figure 12) show that the convergence is not reached at a charge density cutoff of 280 Ry. Use of a larger cutoff of 500 Ry improves the obtained curves though the purely repulsive configuration remains problematic. The origin of this effect is the relative position of the monomers with respect to the discrete real-space grid used to integrate the exchange-correlation energy density. To correct this spurious numerical effect, we have used the NN50 smoothing method implemented in QUICKSTEP.[47] This amounts to evaluate the exchange correlation functional averaged density over grid elements by employing a nearest neighbors smoothing operator, S^q, acting on the density and defined as (Eq. (18) of Ref. 47):

$$(S^q f)_{i,j,k} = \frac{q^3}{q^3 + 6q^2 + 12q + 8} \times \sum_{l=-1}^{1} \sum_{m=-1}^{1} \sum_{n=-1}^{1} q^{-|l|-|m|-|n|} f_{i+l,j+m,k+n}. \quad \text{(A1)}$$

The obtained interaction energy curves are smoothed and identical at both charge-density cutoffs (Figure 12). The observed oscillations without smoothing are consistent with the benchmark calculations reported in Ref. 47. Use of smoothing is more important than use of a larger cutoff. We have chosen to use a cutoff of 400 Ry with the NN50 smoothing method in our AIMD simulations.

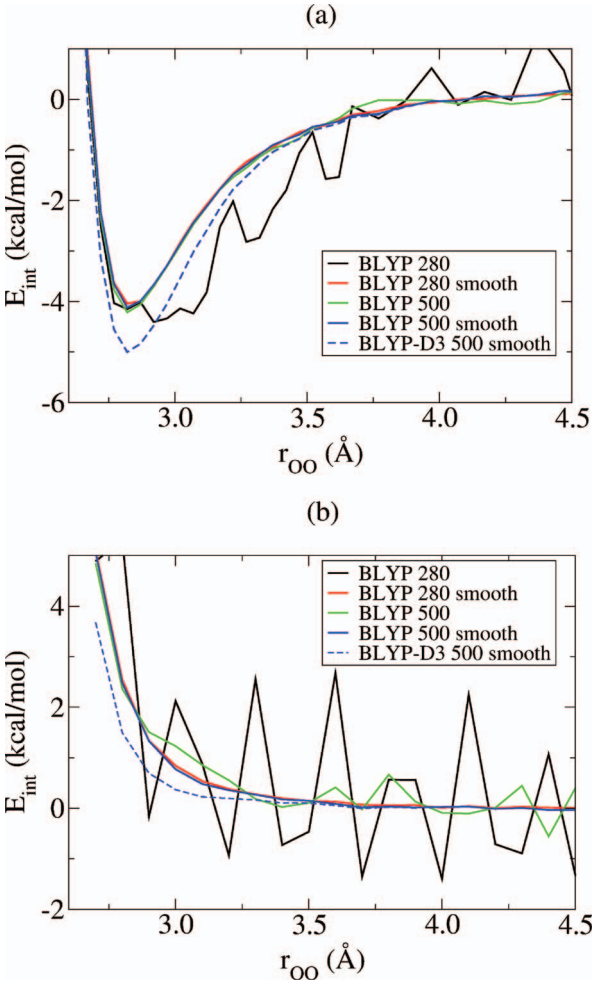

FIG. 12. Interaction energy curves obtained in attractive (a) and purely repulsive (b) configurations of D_2O dimer with a charge density cutoff of 280 and 500 Ry and with or without smoothing (S) method with BLYP and BLYP-D3 functionals.

We now focus on the effect of the Grimme correction on the intermolecular interaction within the dimer. The energy curves show that the interaction with Grimme-D3 correction is more attractive (or less repulsive) up to ~3.6 Å in both configurations (see Figure 12) although the position of the minimum is unchanged. The geometry of the hydrogen-bonded dimer configuration was then fully relaxed: binding energies (E_{int}) of 4.68 and 5.59 kcal mol^{-1} were obtained with BLYP and BLYP-D3, respectively. The difference (0.9 kcal mol^{-1}) compares relatively well with the recent estimation of the London dispersion contribution to the binding energy (1.5 kcal mol^{-1}) obtained from variational Monte Carlo.[64] The BLYP-D3 value is slightly higher yet quite close to previously determined theoretical values (5.02–5.47 kcal mol^{-1}) using other London dispersion correction[37,39,40] and using higher *ab initio* level[64–66] (around 5 kcal mol^{-1}).

[1] B. Guillot, J. Mol. Liq. **101**, 219 (2002).
[2] D. Kennedy and C. Norman, Science **309**, 75 (2005).
[3] D. Asthagiri, L. R. Pratt, and J. D. Kress, Phys. Rev. E **68**, 041505 (2003).
[4] J. C. Grossman, E. Schwegler, E. W. Draeger, F. Gygi, and G. Galli, J. Chem. Phys. **120**, 300 (2004).

[5]E. Schwegler, J. C. Grossman, F. Gygi, and G. Galli, J. Chem. Phys. **121**, 5400 (2004).
[6]M. V. Fernández-Serra and E. Artacho, J. Chem. Phys. **121**, 11136 (2004).
[7]I. W. Kuo, C. J. Mundy, M. J. McGrath, J. I. Siepmann, J. VandeVondele, M. Sprik, J. Hutter, B. Chen, M. L. Klein, F. Mohamed, M. Krack, and M. Parrinello, J. Phys. Chem. B **108**, 12990 (2004).
[8]M. V. Fernández-Serra, G. Ferlat, and E. Artacho, Mol. Simul. **31**, 361 (2005).
[9]J. VandeVondele, F. Mohamed, M. Krack, J. Hutter, M. Sprik, and M. Parrinello, J. Chem. Phys. **122**, 014515 (2005).
[10]P. H. Sit and N. Marzari, J. Chem. Phys. **122**, 204510 (2005).
[11]M. J. McGrath, J. I. Siepmann, I. W. Kuo, C. J. Mundy, J. VandeVondele, J. Hutter, F. Mohamed, and M. Krack, J. Phys. Chem. A **110**, 640 (2006).
[12]H. Lee and M. E. Tuckerman, J. Chem. Phys. **125**, 154507 (2006).
[13]T. Todorova, A. P. Seitsonen, J. Hutter, I. W. Kuo, and C. J. Mundy, J. Phys. Chem. B **110**, 3685 (2006).
[14]H. Lee and M. E. Tuckerman, J. Chem. Phys. **126**, 164501 (2007).
[15]M. Guidon, F. Schiffmann, J. Hutter, and J. VandeVondele, J. Chem. Phys. **128**, 214104 (2008).
[16]J. Schmidt, J. VandeVondele, I. W. Kuo, D. Sebastiani, J. I. Siepmann, J. Hutter, and C. J. Mundy, J. Phys. Chem. B **113**, 11959 (2009).
[17]S. Yoo, X. C. Zeng, and S. S. Xantheas, J. Chem. Phys. **130**, 221102 (2009).
[18]B. Chen, I. Ivanov, M. L. Klein, and M. Parrinello, Phys. Rev. Lett. **91**, 215503 (2003).
[19]J. A. Morrone and R. Car, Phys. Rev. Lett. **101**, 017801 (2008).
[20]Y. Zhao and D. G. Truhlar, Acc. Chem. Res. **41**, 157 (2008).
[21]Y. Andersson, D. C. Langreth, and B. I. Lundqvist, Phys. Rev. Lett. **76**, 102 (1996).
[22]M. Dion, H. Rydberg, E. Schröder, D. C. Langreth, and B. I. Lundqvist, Phys. Rev. Lett. **92**, 246401 (2004).
[23]M. Dion, H. Rydberg, E. Schröder, D. C. Langreth, and B. I. Lundqvist, Phys. Rev. Lett. **95**, 109902 (2005).
[24]D. C. Langreth, M. Dion, H. Rydberg, E. Schröder, P. Hyldgaard, and B. I. Lundqvist, Int. J. Quantum Chem. **101**, 599 (2005).
[25]T. Sato, T. Tsuneda, and K. Hirao, Mol. Phys. **103**, 1151 (2005).
[26]K. A. Maerzke, G. Murdachaew, C. J. Mundy, G. K. Schenter, and J. I. Siepmann, J. Phys. Chem. A **113**, 2075 (2009).
[27]P. L. Silvestrelli, Phys. Rev. Lett. **100**, 053002 (2008).
[28]P. L. Silvestrelli, K. Benyahia, S. Grubisiĉ, F. Ancilotto, and F. Toigo, J. Chem. Phys. **130**, 074702 (2009).
[29]M. Elstner, P. Hobza, T. Frauenheim, S. Suhai, and E. Kaxiras, J. Chem. Phys. **114**, 5149 (2001).
[30]Q. Wu and W. Yang, J. Chem. Phys. **116**, 515 (2002).
[31]S. Grimme, J. Comput. Chem. **25**, 1463 (2004).
[32]S. Grimme, J. Comput. Chem. **27**, 1787 (2006).
[33]P. Jurečka, J. Černý, P. Hobza, and D. R. Salahub, J. Comput. Chem. **28**, 555 (2007).
[34]S. Grimme, J. Antony, S. Ehrlich, and H. Krieg, J. Chem. Phys. **132**, 154104 (2010).
[35]O. A. von Lilienfeld, I. Tavernelli, U. Rothlisberger, and D. Sebastiani, Phys. Rev. Lett. **93**, 153004 (2004).
[36]I. Lin, M. D. Coutinho-Neto, C. Felsenheimer, O. A. von Lilienfeld, I. Tavernelli, and U. Rothlisberger, Phys. Rev. B **75**, 205131 (2007).
[37]P. L. Silvestrelli, Chem. Phys. Lett. **475**, 285 (2009).
[38]A. K. Kelkkanen, B. I. Lundqvist, and J. K. Norskov, J. Chem. Phys. **131**, 046102 (2009).
[39]G. Murdachaew, C. J. Mundy, and G. K. Schenter, J. Chem. Phys. **132**, 164102 (2010).
[40]I. Lin, A. P. Seitsonen, M. D. Coutinho-Neto, I. Tavernelli, and U. Rothlisberger, J. Phys. Chem. B **113**, 1127 (2009).
[41]V. Weber, S. Merchant, P. D. Dixit, and D. Asthagiri, J. Chem. Phys. **132**, 204509 (2010).
[42]J. Wang, G. Román-Pérez, J. M. Soler, E. Artacho, and M. Fernández-Serra, J. Chem. Phys. **134**, 024516 (2011).
[43]S. Yoo and S. S. Xantheas, J. Chem. Phys. **134**, 121105 (2011).
[44]A. D. Becke, Phys. Rev. A **38**, 3098 (1988).
[45]C. Lee, W. Yang, and R. G. Parr, Phys. Rev. B **37**, 785 (1988).
[46]G. Lippert, J. Hutter, and M. Parrinello, Mol. Phys. **92**, 477 (1997).
[47]J. VandeVondele, M. Krack, F. Mohamed, M. Parrinello, T. Chassaing, and J. Hutter, Comput. Phys. Commun. **167**, 103 (2005).
[48]See http://cp2k.berlios.de/ for CP2K.
[49]S. Goedecker, M. Teter, and J. Hutter, Phys. Rev. B **54**, 1703 (1996).
[50]C. Hartwigsen, S. Goedecker, and J. Hutter, Phys. Rev. B **58**, 3641 (1998).
[51]J. L. F. Abascal and C. Vega, J. Chem. Phys. **123**, 234505 (2005).
[52]See http://www.cse.scitech.ac.uk/ccg/software/DL_POLY/ for DL_POLY.
[53]A. K. Soper, Chem. Phys. **258**, 121 (2000).
[54]R. Mills, J. Phys. Chem. **77**, 685 (1973).
[55]K. Yoshida, C. Wakai, N. Matubayasi, and M. Nakahara, J. Chem. Phys. **123**, 164506 (2005).
[56]K. R. Harris and L. A. Woolf, J. Chem. Soc., Faraday Trans. **76**, 377 (1980).
[57]G. Palinkas, P. Bopp, G. Jancso, and K. Heinzinger, Z. Naturforsch., A: Phys. Sci. **39**, 179 (1984).
[58]A. M. Saitta and F. Datchi, Phys. Rev. E **67**, 020201 (2003).
[59]A. M. Saitta, T. Strässle, G. Rousse, G. Hamel, S. Klotz, R. Nelmes, and J. Loveday, J. Chem. Phys. **121**, 121 (2004).
[60]M. Bernabei, A. Botti, F. Bruni, M. A. Ricci, and A. K. Soper, Phys. Rev. E **78**, 021505 (2008).
[61]M. Bonetti, G. Romet-Lemonne, P. Calmettes, and M.-C. Bellissent-Funel, J. Chem. Phys. **112**, 268 (2000).
[62]See http://webbook.nist.gov for NIST webbook of chemistry.
[63]W. J. Lamb, J. Chem. Phys. **74**, 6875 (1981).
[64]F. Sterpone, L. Spanu, L. Ferraro, S. Sorella, and L. Guidoni, J. Chem. Theor. Comput. **4**, 1428 (2008).
[65]W. Klopper, J. G.C.M. van Duijneveldt-van de Rijdt, and F. B. van Duijneveldt, Phys. Chem. Chem. Phys. **2**, 2227 (2000).
[66]B. Santra, A. Michaelides, and M. Scheffler, J. Chem. Phys. **127**, 184104 (2007).